IOP Conf. Series: Materials Science and Engineering **114** (2016) 012115 doi:10.1088/1757-899X/114/1/012115

Analysis of fatigue crack propagation behaviour in SiC particulate Al_2O_3 whisker reinforced hybrid MMC

AKM Asif Iqbal[1], Yoshio Arai[2]

[1]Faculty of Manufacturing Engineering, Universiti Malaysia Pahang, 26600 Pekan, Pahang, Malaysia
[2]Division of Mechanical Engineering and Science, Graduate School of Science and Engineering, Saitama University, 338-8570, Japan

asifiqbal@ump.edu.my

Abstract. The fatigue crack propagation behaviour of a cast hybrid metal matrix composite (MMC) was investigated and compared with the crack propagation behaviour of MMC with Al_2O_3 and Al alloy in this article. Three dimensional (3D) surface analysis is carried out to analyze the crack propagation mechanism. All three materials clearly show near threshold and stable crack growth regions, but the rapid crack growth region is not clearly understood. The crack propagation resistance is found higher in hybrid MMC than that of MMC with Al_2O_3 whisker and the Al alloy in the low ΔK region. The crack propagation in the hybrid MMC in the near-threshold region is directed by the debonding of reinforcement–matrix followed by void nucleation in the Al alloy matrix. Besides, the crack propagation in the stable- or mid-crack-growth region is controlled by the debonding of particle–matrix and whisker–matrix interface caused by the cycle-by-cycle crack growth along the interface. The transgranular fracture of the reinforcement and void formation are also observed. Due to presence of large volume of inclusions and the microstructural inhomogeneity, the area of striation formation is reduced in the hybrid MMC, caused the unstable fracture.

Keywords: Metal matrix composites (MMCs), Fatigue crack propagation, Stress intensity factor, 3D analysis, Fracture.

1. Introduction

The development of metal matrix composites (MMCs) has set the stage for a new revolution in materials. These composites have attracted significant research interest in the past few decades owing to their exceptionally high specific strength, Stiffness, fatigue and wear resistance. The presence of the reinforcement phase in a continuous metal matrix result in properties not attainable by other means, thereby enhancing the potential range of possible applications in the automobile and aerospace industries [1].

Many experimental and numerical studies have been conducted to determine the fatigue crack propagation behaviour of a variety of aluminium alloys reinforced with either particulates or whiskers [2-9]. These studies reported that the crack growth behavior in particle reinforced MMCs is very much

[1] asifiqbal@ump.edu.my

dependent on reinforcement characteristics [10, 11], and on matrix microstructure [4, 5]. The most pronounced effects of reinforcement on fatigue crack growth are in the threshold region, where crack closure processes predominate, and at high stress-intensity levels, where growth rates accelerates rapidly. In general, composite materials exhibit higher threshold values in the stress intensity factor range, ΔK_{th}, as compared to their corresponding monolithic materials. Shang and Ritchie [12] explained this behaviour that at low applied ΔK where particle fracture is less likely, coarser SiC particles improved nominal fatigue thresholds, ΔK_{th} of Al-MMCs due to enhanced roughness-induced closure. Chawla et al. [13] have reported that higher ΔK_{th} can be obtained by increasing volume fraction and decreasing particle size of the reinforcements. Mechanisms responsible for this behaviour were explained in terms of load transfer from the matrix to the high stiffness reinforcement, increasing obstacles for dislocation motion and the decrease in strain localization with decreasing inter-particle spacing as a result of reduced particle size. Besides, The Paris law slope of da/dN versus ΔK curve for the composites can be compared to that of unreinforced alloys, although at very high ΔK, the crack propagation in the composites is much higher. Botstein et al. [14] measured higher crack growth rates in the mid-growth rate (Paris Law) regime compared to the monolithic alloy while doing experiment with Al 2014-40% SiC_p and Al 7091-30% SiC_p composites. This is due to lower fracture toughness of the composite, relative to the unreinforced alloy. The effect of particle clustering on fatigue crack propagation in MMC has been investigated and explained that particle clustering significantly increased crack growth in the mid-growth rate (Paris Law) regime [14, 15]. Moreover, the effect of load ratio on crack propagation behavior of MMCs has also been investigated [5, 16]. In general, an increase in load ratio (positive R-ratio) resulted in a decrease in threshold stress intensity. Crack closure was generally considered to be the primary reason for the effect of load ratio on fatigue threshold. Besides, few studies have pointed out the effect of whisker reinforcement on fatigue crack growth. The orientation of whisker plays a vital role in advancing fatigue crack. Mason and Ritchie [17] observed higher threshold value in whisker reinforced composites compared to particulate reinforced materials when measured along the rolling direction. They attributed the effect to crack tip shielding by whisker pull-out and roughness induced closure. Moreover, Iqbal et al. [18] have investigated that the fracture of cast whiskers reinforced composites due to cyclic loading was dominated by the interfacial debonding of whisker-matrix followed by the void nucleation and coalescence in the Al alloy matrix.

Many of the crack propagation studies reported above have been performed either particulate or whisker reinforced systems. A few studies have been reported recently explained the crack behaviour and fatigue damage behavior of hybrid MMCs. Oh and Han [19] have demonstrated that increasing particle contents increased the fatigue threshold (ΔK_{th}) in hybrid MMC reinforced with Al_2O_3 particles and Al_2O_3 fibers means the hybrid reinforcement composites provide better control of damage tolerance properties over conventional particle reinforced composites. Besides, the authors of this article have investigated the fatigue crack initiation mechanism in a cast hybrid MMC and observed that the microcracks formed at the reinforcement/matrix interface in very early stage of the fatigue life [18]. While these studies explained the fatigue responses, the underlying mechanism of crack propagation and damage nucleation during fatigue remain unclear and needs further analysis to provide better understanding of using this material in large scale structural applications e.g., the brake disc of a high speed railway coach.

In the present study the crack propagation and growth behavior during fatigue was investigated in three different types of materials: cast hybrid MMC (SiC_p + Al_2O_3 whiskers), cast MMC reinforced with Al_2O_3 whiskers, and unreinforced cast Al alloy. The results are discussed through the comparison of the observed mechanisms in the three materials.

Table 1. Chemical composition of AC4CH alloy, (wt%)

Si	Fe	Mg	Ti	Al
7.99	0.2 (max.)	0.57	0.07	Bal.

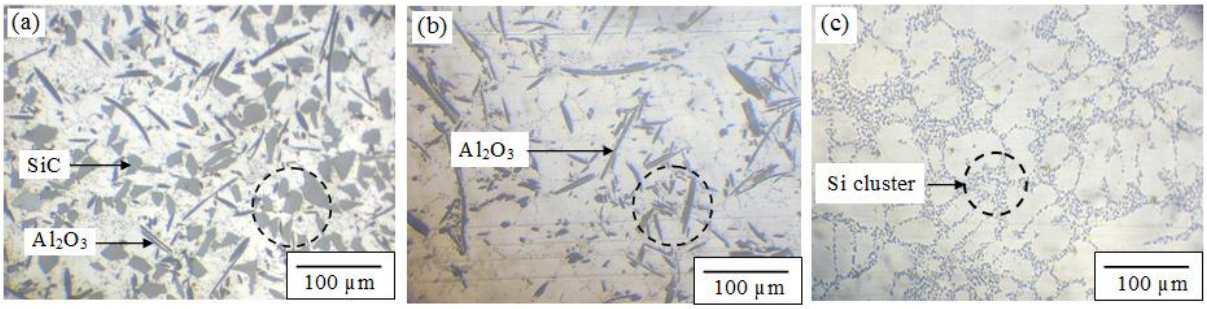

Figure 1. Microstructure (a) Hybrid MMC, (b) MMC with Al_2O_3 whiskers and (c) Al alloy

2. Materials and experimental procedure

The materials used in this study were an aluminum alloy JIS-AC4CH [20], whisker reinforced MMC (JIS AC4CH alloy with 9 vol% Al_2O_3 whiskers) and hybrid MMC (JIS AC4CH alloy with 21 vol% SiC particles and 9 vol% Al_2O_3 whiskers as reinforcements). The chemical composition of the Al alloy is shown in Table-1. The MMC materials were fabricated by the squeeze casting process. Hybrid preform of SiC particles and Al_2O_3 whiskers was used for the fabrication of hybrid MMC while a preform of Al_2O_3 whiskers was used for MMC with Al_2O_3 whisker. The 100 MPa pressure was maintained during squeeze casting process to press the melt into all the open pores of the hybrid perform and to overcome the resistance against flow. Finally, all the materials were heat treated by using the T7 process. The microstructure of the materials is shown in Fig. 1. The SiC particles embedded in the hybrid MMC were mostly rectangular (Fig. 1a) while the Al_2O_3 whiskers in both MMC materials were roller-shaped (Fig. 1a and 1b). The average length of SiC particles and Al_2O_3 whiskers was 23 µm and 35 µm respectively. The average diameter of the Al_2O_3 whiskers was 2 µm in both MMCs. In the Al alloy, the average grain size was found to be 48 µm. The Si particles in the Al alloy were round with an average diameter of 3 µm. Cluster of reinforcement particles and whiskers were observed at frequent intervals in both the MMC materials, as indicated by the circles in Fig. 1a and 1b. In the Al alloy, cluster of Si was also observed, as shown by the circle in Fig. 1c.

To investigate and analyze the crack growth behaviour and damage nucleation, single-edge notched specimens with dimension of 100 mm length, 6 mm thickness, 8 mm width and 0.5 mm notch width were used. All the specimens were polished by using the polishing machine with 15, 3, and 1 µm diamond particles sequentially to completely remove the scratches and surface machining marks. Conventional three point bending fatigue tests were carried out in a Shimazu ServoPulser. The fatigue tests were performed at constant load ratio, R = 0.1 using a sinusoidal wave form under ΔK control mode. A decreasing ΔK procedure was used to determine the threshold stress intensity as per ASTM E647 [21]. ΔK was reduced in decrements not greater than 5%. The stress intensity corresponding to a crack growth rate of 10^{-11} m/cycle was taken as the threshold stress intensity, ΔK_{th}. Once the threshold stress intensity was determined, the crack growth was continued by increasing ΔK in increments not greater than 5%. Crack propagation behavior and growth was measured using a Bioden replicating films softened in acetone. The fracture surfaces of the specimens were observed by scanning electron microscopy (SEM). The regions which correspond to ΔK in the near threshold region and the stable crack growth region were examined. Moreover, the roughness of the fracture surface was examined by using the three-dimensional (3D) Mex software.

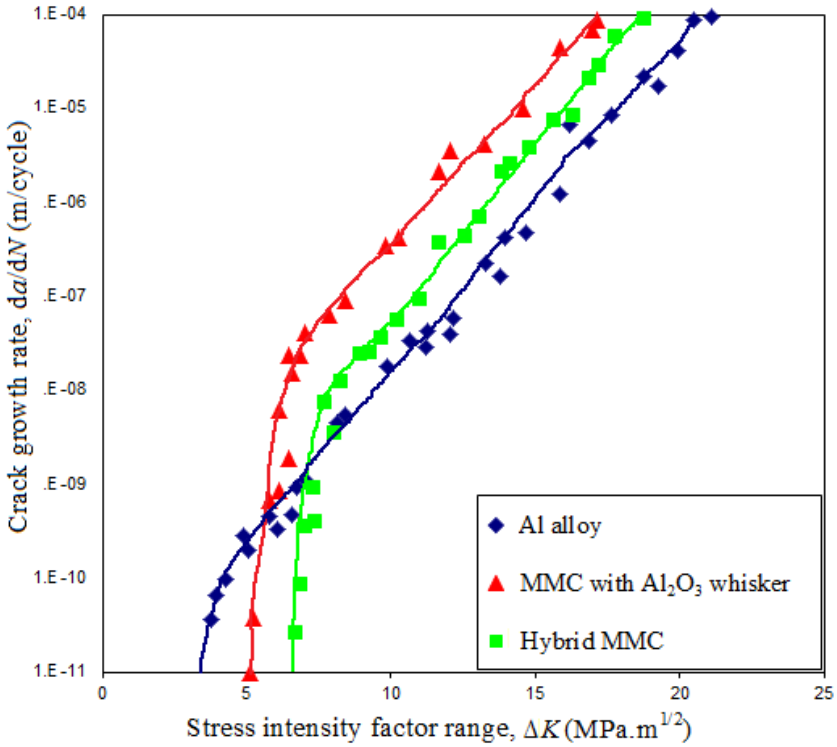

Figure 2. Fatigue crack growth behaviour of hybrid MMC, MMC with Al_2O_3 whisker, and Al alloy at load ratio $R = 0.1$

3. Result and discussion

The fatigue crack growth behavior of the three materials is presented in Figure 2. The figure clearly shows near threshold and stable crack growth regions, but the rapid crack growth region is not clearly understood. The two composites show different behaviors from the matrix alloy. The hybrid MMC shows a higher threshold stress intensity ΔK_{th} as compared to the MMC with Al_2O_3 and Al alloy. The higher value of ΔK_{th} for the hybrid MMC can be ascribed to the high modulus of the composite, results in a lower crack-tip opening displacement for a given applied stress intensity factor ΔK . These results are consistent with data in the literature [22, 23]. In the case of MMC with Al_2O_3 whisker, the crack growth rate (da/dN) is higher than that of monolithic matrix alloy in the stable crack growth region. Moreover, the both composites show higher Paris-law slope compared to the unreinforced Al alloy. This higher value of the Paris-law slope can be attributed due to the low fracture toughness of the composites relative to the unreinforced alloy. Besides, the hybrid MMC exhibits better crack growth resistance during fatigue as compared to MMC with Al_2O_3 over the entire stress intensity range.

Figure 3 demonstrates the matching fracture surface at the near threshold and stable-crack-growth region and corresponding three dimensional (3D) surface analysis of crack propagation from one SiC particle to another SiC particle at the near-threshold and stable-crack-growth regions. The particle-matrix interfacial debonding (indicated by SiC-1/Al-alloy-1 pair) and the void nucleation are observed in the near threshold region. However, the particle-matrix interfacial debonding (indicated by the SiC-4/Al-alloy-4), particle fracture (indicated by SiC-3/SiC-3) and void nucleation are observed in the stable crack growth region. During cyclic loading, the reinforcing particles deformed elastically within the plastically deforming matrix alloy in the hybrid MMC. Moreover, the edges of the stiff ceramic reinforcements acted as stress concentrators, localizing the plastic strain between the particles and the matrix. Thus, a large strain mismatch occurred between the SiC particles and the Al matrix. Under these conditions, the stress became too high on the particle–matrix interface and debonding occurred. Moreover, very few striation marks are observed in the stable crack growth region.

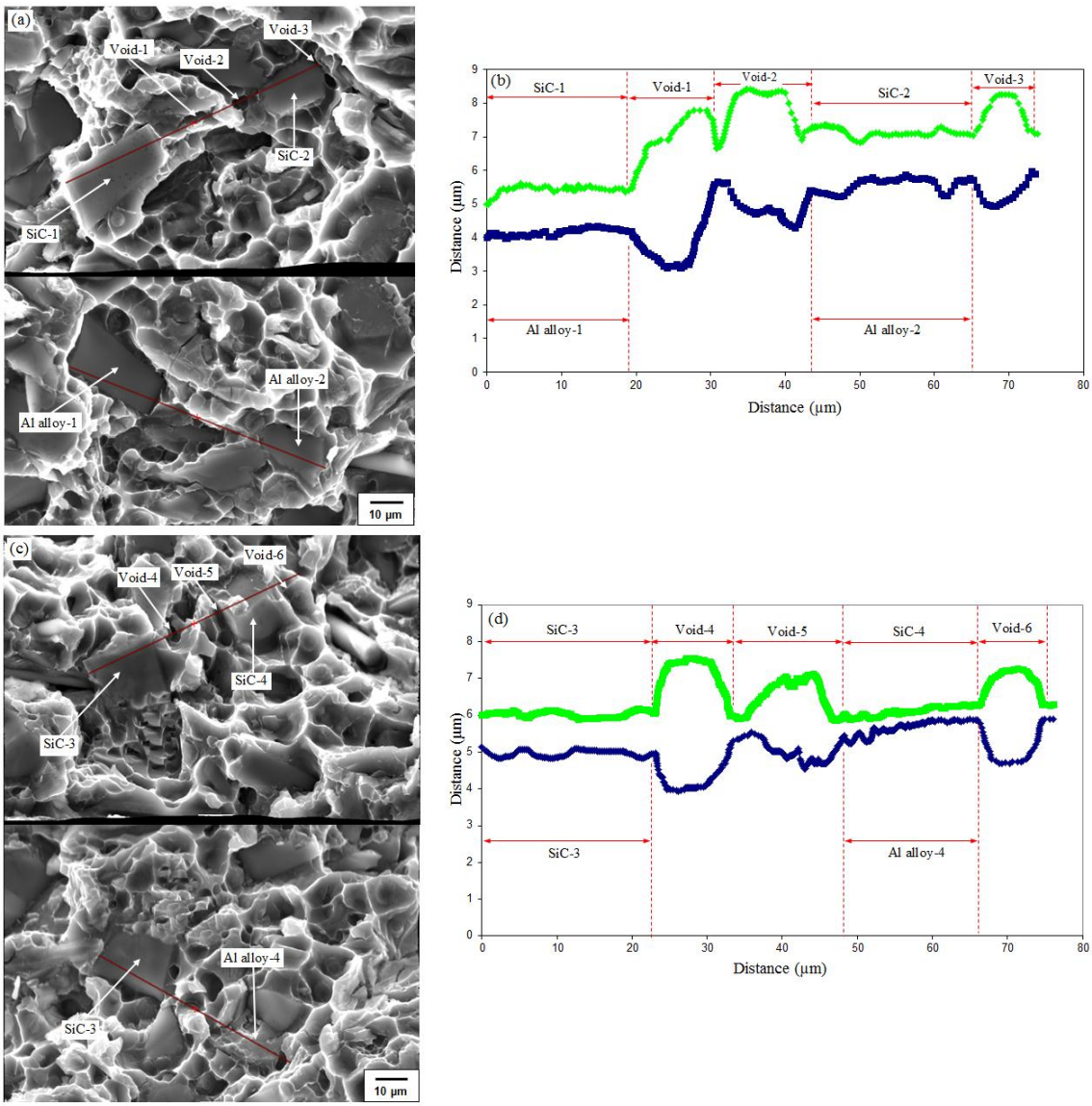

Figure 3. Crack propagation from one SiC particle to another SiC particle in hybrid MMC: (a) Matching fracture surface at the near threshold region, (b) Crack surface profile at the near threshold region, (c) Matching fracture surface at the stable crack growth region, (d) Crack surface profile at the stable crack growth region.

Due to the presence of large 30 vol% of reinforcement, inter-reinforcement spacing in hybrid MMC is very small. Thus, the striation forms in very limited area. The average spacing of the striation is calculated to be 1.2 μm, which is very close to the da/dN value of 1 μm/cycle at this stage. The submicron roughness on the debonded particle–matrix interface is clearly observed in the crack surface profile of Fig. 3b (indicated by SiC-1/ Al alloy-1 pair and SiC-2/Al alloy-2 pair in Fig 3b). The edge of the dimple corresponds to the edge of the debonded interface, which means that the voids between the SiC–Al interfaces grow until they coalesce with the interfacial crack at the near threshold region. As illustrated in Fig. 3d, the crack path in the stable crack growth region is relatively flat with the transgranular fracture of the SiC particles (SiC-3/SiC-3 pair) as the value of ΔK increased. Moreover, the interfacial fracture between SiC-4 and Al alloy-4, indicated as a cross-sectional shape in Fig. 3d, shows cyclic roughness, with an interval having the same order of magnitude as the crack

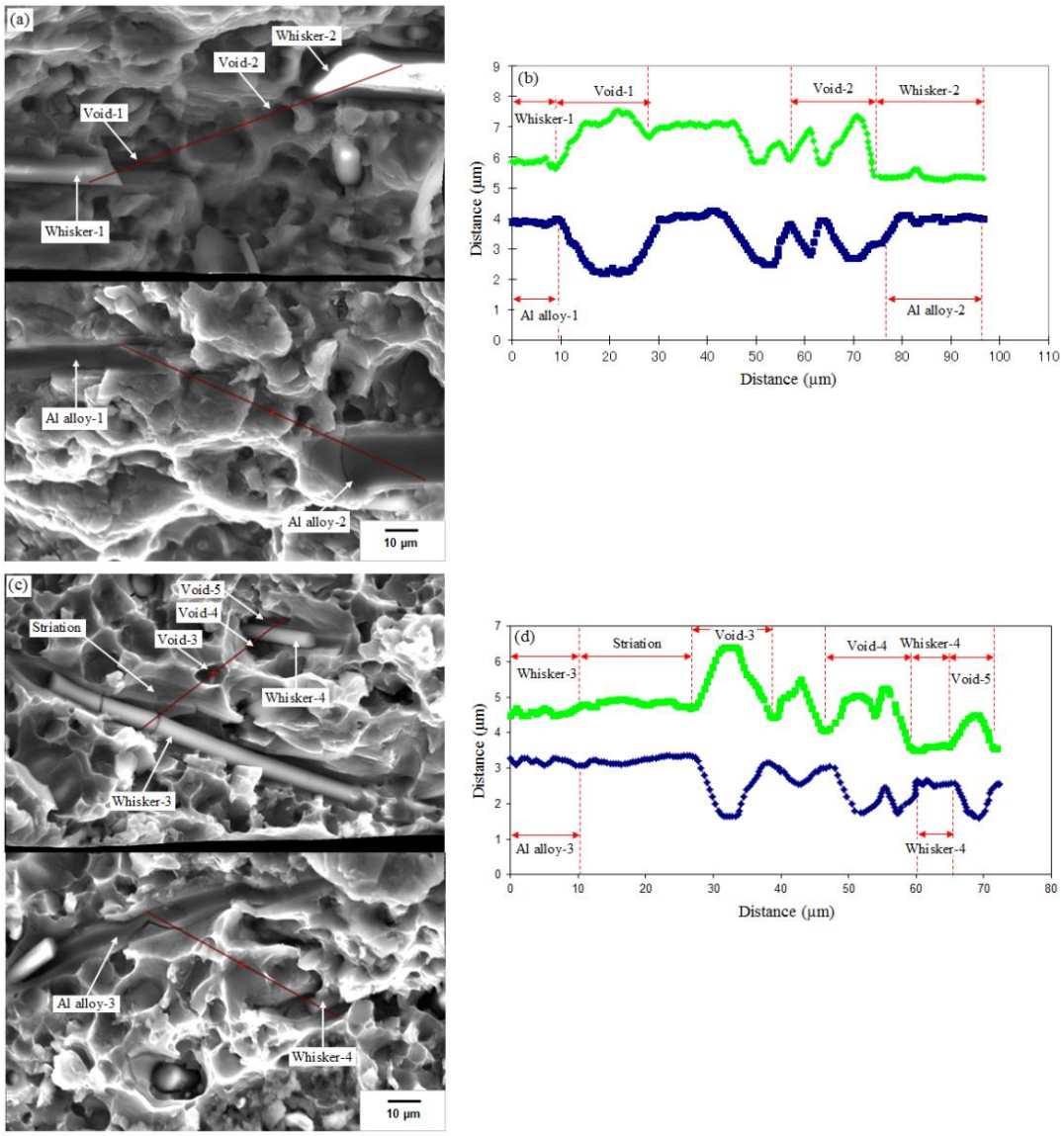

Figure 4. Crack propagation from one Al_2O_3 whisker to another in MMC with Al_2O_3 whisker: (a) Matching fracture surface at the near threshold region, (b) Crack surface profile at the near threshold region, (c) Matching fracture surface at the stable crack growth region, (d) Crack surface profile at the stable crack growth region.

growth rate in this region. This means that the crack propagated cycle-by-cycle at the interface, pointing that debonding took place over a number of cycles. The matching fracture surface in the near threshold region and stable crack growth region of MMC with Al_2O_3 whisker and corresponding three dimensional (3D) surface analysis of crack propagation from one Al_2O_3 whisker to another Al_2O_3 whisker is presented in Fig. 4. The debonding of the whisker–matrix interface (indicated by Whisker-1/ Al alloy-1 pair and Whisker-2/Al alloy-2 pair) and void nucleation are observed in the near-threshold region. The dimple surface connects the interval between the interfacial fractures (Fig. 4b). However, the transgranular fracture of the whisker (indicated by Whisker-4/Whisker-4 pair) and the debonding of the whisker–matrix interface (indicated by Whisker-3/Al alloy-3 pair) are observed in the stable-crack-growth region. A significant number of the striation marks are also observed in this

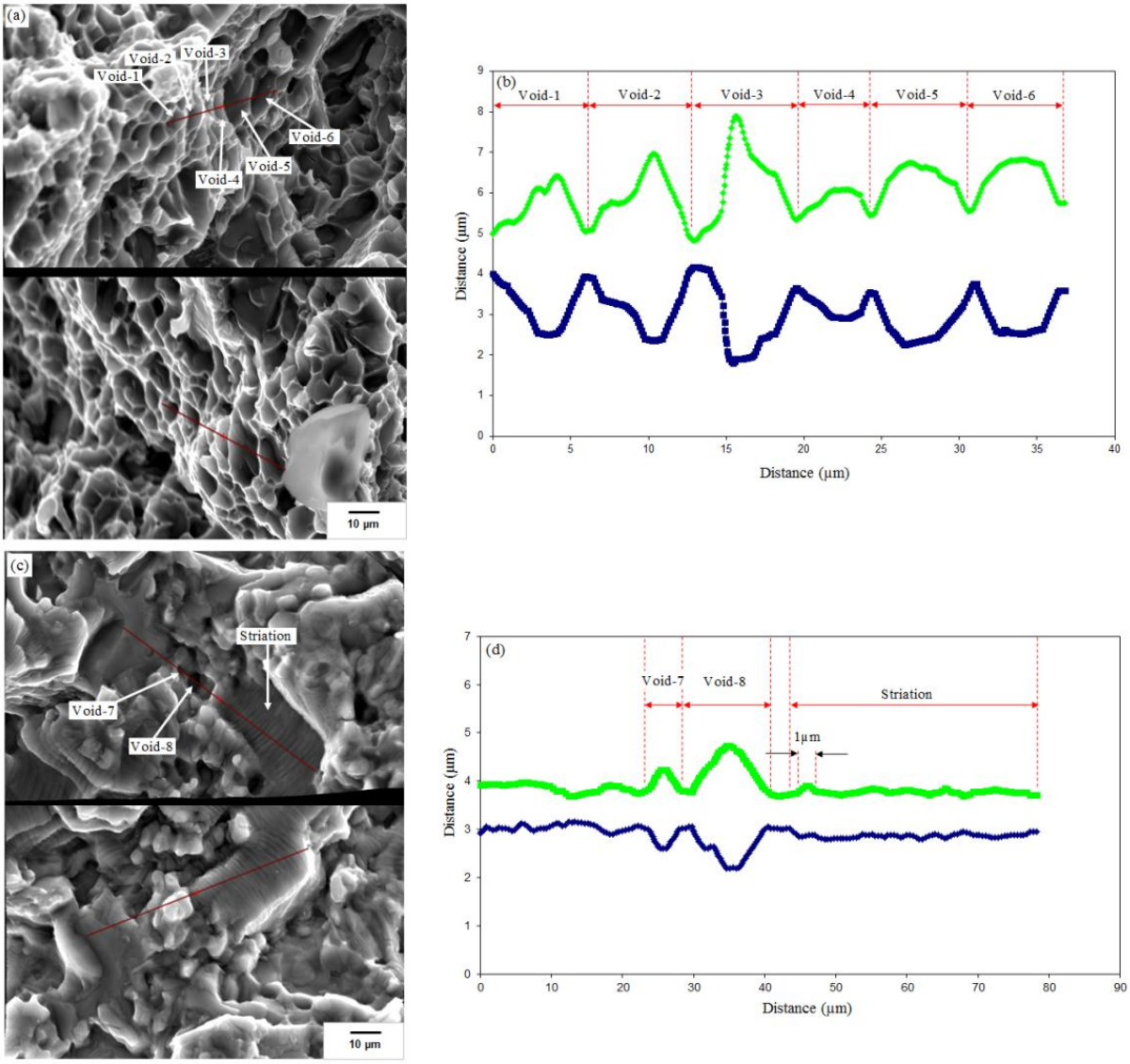

Figure 5. Ccrack propagation in Al alloy: (a) Matching fracture surface at the near threshold region, (b) Crack surface profile at the near threshold region, (c) Matching fracture surface at the stable crack growth region, (d) Crack surface profile at the stable crack growth region

region. Due to the presence of 9 vol% of whiskers, inter-reinforcement spacing is reasonably large and relatively large Al grains are present than that of hybrid MMC. Thus striation morphologies are formed. The striation morphology on the whisker–Al matrix interface continues into the Al matrix (Whisker-3/Al alloy-3 pair and Striation in Fig. 4d) and reaches the voids (Void-3 and Void-4). The interval of the cyclic roughness of the interfacial fracture between whisker-3/Al alloy-3 shows the same order of magnitude as the crack growth rate at this stage. This means that the crack grew on the interface over a number of cycles, causing debonding of the interface. These results indicate that at lower ΔK values, fatigue crack propagation and growth is controlled by debonding of the whisker–matrix interface and void nucleation and coalescence in the Al alloy matrix. However, at higher ΔK values, the crack growth is controlled by debonding of the whisker–matrix interface caused by the cycle-by-cycle crack growth on the interface, as well as whisker fracture followed by striation formation and void nucleation in the Al matrix. Figure 5 represents the matching fracture surface in

the near threshold region and stable crack growth region of Al alloy and corresponding three dimensional (3D) surface analysis of crack propagation. The crack surface profile of both regions clearly demonstrates that the cracks propagated by void nucleation and coalescence in the near-threshold region (Fig. 5a and 5b) and by striation formation, as well as void nucleation in the stable-crack-growth region (Fig. 5c and 5d). In the Al alloy, large Al grains are present. Because of the presence of large Al grains, multiple slip system operates in the stable crack growth region. Subsequently, striation morphologies form into large Al grains along the crack propagation path during cyclic loading. The average spacing of the striations in this region was calculated to be 1 μm, which is exactly the same value of da/dN at this stage. The interval of the cyclic roughness in the striation morphology shown in Fig. 5d indicates that the crack with striation formation penetrated the voids, which means that the two striation facets were formed followed by the void nucleation and coalescence.

From the above fracture surface and three dimensional (3D) surface analysis, it is evident that the fatigue crack propagation behavior and damage development in three materials are strikingly different. It appears that reinforcement debonding is the dominant mechanism of crack growth in the near threshold region for both composite materials. The fatigue crack growth in the near threshold region is generally explained in terms of the crack closure [24]. Several variables, including crack surface roughness, yield strength and elastic modulus are known to influence crack closure and the value of the fatigue threshold (ΔK_{th}) [24, 25]. Owing to the presence of both SiC particles and Al_2O_3 whiskers in hybrid MMC, modulus mismatch occurs between the particles, whiskers, and matrix. Hence, the interface debonding between the SiC particles and the Al alloy matrix is very frequently observed in the near-threshold region, leads to an increased surface roughness than that of other two materials. Subsequently, the fatigue threshold ΔK_{th} in the hybrid MMC increased. It is also apparent from the 3D surface analysis that the crack growth in the stable- or mid–crack-growth region is directed by the particle and whisker debonding from the matrix caused by the cycle-by-cycle crack growth on the interface and particle fractures in the hybrid MMC. It has been stated that when the plastic zone is much larger than the size of the particles, particle fracture may take place [24]. Owing to the presence of large volumes of inclusion in the hybrid MMC, the area of striation formation is reduced. The lack of striation formation, thus increases the crack propagation rate in hybrid MMC, results unstable fracture.

4. Conclusions

The crack propagation behavior due to cyclic loading in hybrid MMC were investigated. The study focused on the crack growth behavior at the near-threshold and stable-crack-growth regions of a hybrid MMC and compared the behavior of crack growth in MMC with Al_2O_3 whiskers, and Al alloy. The following conclusions are made:

(1) The hybrid MMC shows better fatigue crack growth resistance than MMC with Al_2O_3 whisker and the Al alloy in the low ΔK region.

(2) The crack growth of the hybrid MMC in the near-threshold region is directed by the debonding of reinforcement–matrix followed by void nucleation in the Al alloy matrix. Besides, the crack growth value in the stable- or mid-crack-growth region is controlled by the debonding of particle–matrix and whisker–matrix interface caused by the cycle-by-cycle crack growth along the interface, as well as by the transgranular fracture of particles and whiskers. Large volume of inclusion and microstructural inhomogeneity leads to the lack of striation formation area in hybrid MMC, caused the unstable fracture.

References

[1] Miracle DB. (2005). Metal matrix composites – from science to technological significance. Compos Sci Technol;65:2526–40.
[2] Kaynak C, Boylu S. (2006). Effect of particulates on the fatigue behaviour of an Al-alloy matrix composite. Mater Des;27:776–82.
[3] Iqbal AA, Arai Y, Araki W. (2014). Fatigue crack growth mechanism in cast hybrid metal matrix composite reinforced with SiC particles and Al_2O_3 whiskers. Trans Nonferrous Met Soc China;24:1–13.
[4] Sugimura Y, Suresh S. (1992). Effects of SiC content of fatigue crack growth in aluminum alloys reinforced with SiC particles. Metall Trans A;23:2231–42.
[5] Chawla N, Ganesh VV. (2010). Fatigue crack growth of SiC particle reinforced metal matrix composites. Int J Fatigue;32:856–63.
[6] Chen ZZ. Tokaji K. (2004). Effects of particle size on fatigue crack initiation and small crack growth in SiC particulate reinforced aluminium alloy composites. Mater Lett;58:2314-21
[7] Wang Z, Zhang RJ. (1994). Microscopic characteristics of fatigue crack propagation in aluminum alloy based particulate reinforced metal matrix composites. Acta Metall;42:1433–45.
[8] Liu G, Shang JK. (1996). Fatigue crack tip opening behavior in particulate reinforced Al alloy composites. Acta Metall;44:79–91.
[9] Crawford BR, Griffiths JR. (1999). Role of reinforcement particles during fatigue cracking of a micral-20-reinforced 6061 alloy. Fatigue Fract Eng Mater Struct;22:811–20.
[10] Llorca J. (2002). Fatigue of particle and whisker reinforced metal matrix composites. Prog Mater Sci;47:283–353.
[11] Llorca J, Ruiz J, Healy JC, Elices M, Beevers CJ.(1994). Fatigue crack propagation in salt water, air and high vacuum in a spray-formed particulate-reinforced metal matrix composite. Mater. Sci. Eng. A;185:1-15.
[12] Shang JK, Ritchie RO. (1989). On the particle-size dependence of fatigue-crack propagation thresholds in SiC-particulate-reinforced aluminum-alloy composites: role of crack closure and crack trapping. Acta Metall;37:2267–78.
[13] Chawla N, Andres C, Jones JW, Allison JE.(1998). Effect of SiC volume fraction and particle size on the fatigue resistance of a 2080 Al/SiC_p composite. Metall Mater Trans A; 29A: 2843-54
[14] Botstein O, Arone R, Shpigler B. (1990). Fatigue crack growth mechanisms in Al-SiC particulate metal matrix composites. Mater Sci Eng A;128: 15.
[15] Bruzzi MS, McHugh PE. (2004). Micromechanical investigation of the fatigue crack growth behaviour of Al-SiC MMCs. Int J Fatigue;26:795-804.
[16] Hong SJ, Kim HM, Huh D, Surayanarayana C, Chun BS. (2003). Effects of clustering on the mechanical properties of SiC particulate reinforced aluminium alloy 2024 metal matrix composites. Mater Sci Eng A;347:198-204.
[17] Mason JJ, Ritchie RO. (1997). Fatigue crack growth resistance in SiC particulate and whisker reinforced P/M 2124 aluminum matrix composites. Mater Sci Eng A;231:170–182.
[18] Iqbal AA, Arai Y, Araki W. (2013). Effect of hybrid reinforcement on crack initiation and early propagation mechanisms in cast metal matrix composites during low cycle fatigue. Mater des;45:241-52.
[19] Oh KH, Han KS. (2007). Short-fiber/particle hybrid reinforcement: Effects on fracture toughness and fatigue crack growth of metal matrix composites. Compos sci technol;67:1719-26.
[20] 'Aluminium alloy castings', JIS H5202, Japan Industrial Standard 2002
[21] E647-08[S]. ASTM standard 2010
[22] Lukasak DA, Bucci RJ. (1992). Alloy technology Div Rep No. KF-34. Alcoa (PA): Alcoa Technical Center;
[23] Allison JE, Jones JW. In: Suresh S, Mortensen A, Needleman A, editors. (1993). Fundamentals of metal matrix composites. Stoneham (MA): Butterworth-Heinemann; p. 269.

[24] Lawson L, Chen EY, Meshii M. (1999). Near threshold fatigue: a review. Int J of fatigue, 21 (s): 15-34.
[25] Wasen J, Heier E. (1988). Fatigue crack growth thresholds-the influence of young's modulus and fracture surface roughness. Int j of fatigue; 20 (10): 737-42.